ELSEVIER

Catalysis Today 68 (2001) 183–190

CATALYSIS TODAY

www.elsevier.com/locate/cattod

New nickel catalysts supported on highly porous alumina intercalated laponite for methane reforming with CO_2

Kap-Sung Hwang [a], H.Y. Zhu [b,*], G.Q. Lu [b]

[a] *Department of Environmental Engineering, ChungCheong College, Chungbuk 363-792, South Korea*
[b] *Department of Chemical Engineering, The University of Queensland, St. Lucia 4072, Australia*

Abstract

Alumina intercalated laponite (Al-laponite) was prepared with a polyethylene oxide (PEO) surfactant and used as supports of nickel catalysts for the carbon dioxide reforming reaction with methane to synthesis gas. The effects of the supports of intercalated laponite and catalyst preparation on catalytic activity, stability and carbon deposition were investigated for the above reforming reaction. We found that the pore structure of the Al-laponite supports can be tailored with the surfactant and the catalyst with well-developed porosity exhibited higher catalytic activity and a longer time of catalyst stability. © 2001 Elsevier Science B.V. All rights reserved.

Keywords: CO_2 reforming; Nickel catalyst; Intercalated clay; Surfactant template

1. Introduction

The reforming of carbon dioxide with methane has recently received an increasing interest as it can produce gas with a H_2/CO ratio around 1. This reaction also has important environmental implications, since both methane and carbon dioxide are greenhouse gases. Catalytic reforming of carbon dioxide with methane to synthesis gas has been proposed as one of the promising technologies for utilization of these two greenhouse gases as carbon-containing materials. However, no industrial technology has been so far established due to the serious problem of catalyst deactivation [1,2].

It is well known that supported group VIII metals are good catalysts for this reforming reaction. One serious problem is the catalyst deactivation due to carbon deposition, especially for Ni-based catalysts. The development of Ni catalysts with little or no coking deactivation is of great interest to industrial application for carbon dioxide reforming of methane [3].

It has been found that the support and methods of catalyst preparation influence the catalyst activity for carbon dioxide reforming reaction. Clay materials are interesting materials as catalyst support not only due to their great abundance and low cost but also because of their particular properties and structures. By intercalating the parallel silicate layers of swellable clay with particles of various metal oxides, large porosity can be created [4,5]. The pore structure of the intercalated products referred to as pillared interlayered clays depends on the oxide pillars and preparation methods [6]. Furthermore, the surface property of pillared clays can be altered and their pore structure can be fine-turned [7]. The diverse surface nature and the pore structure provides a great potential for these solids to be used as catalysts and adsorbents. In recent years, numerous studies on the catalytic

---

[*] Corresponding author. Tel.: +61-7-3365-3708;
fax: +61-7-3365-4199.
E-mail address: hyzhu@cheque.uq.edu.au (H.Y. Zhu).

PII: S0920-5861(01)00299-1

applications of pillared clays have been reported [8]. In a previous study, we found that the pore structure of pillared clay supports affected the catalyst activity in CO_2 reforming of methane [9]. Mesoporous solid is preferred as a catalyst support for the reforming reaction.

In this paper, we report an investigation on a new class of clay-based Ni-catalyst for carbon dioxide reforming of methane. A synthetic clay, laponite was intercalated with alumina in the presence of a polyethlyene oxide (PEO) surfactant resulting in supports with large porosity [10]. The effects of the surfactant on the textural characteristics of intercalated laponite supports and the catalytic activity and stability of the catalysts for carbon dioxide reforming with methane are studied.

2. Experimental

2.1. Supports preparation

The preparation of alumina intercalated laponite follows the procedures proposed by Zhu et al. [10]. The laponite clay was supplied by Fernz Specialty Chemicals, Australia. The clay powder has a cation exchange capacity (CEC) of 55 meq per 100 g of clay. A commercial solution of aluminum hydroxychloride (Locron L from Hoechst, Germany), which contains polyoxycations of aluminum hydrate, was used as the alumina source. The concentration of aluminum of this solution was given in an Al_2O_3 content of $23.5 + 0.5$ wt.%, the ratio of OH/Al is 2.5 and pH of the solution was about 3.5–3.7. Non-ionic polyethylene oxide (PEO) surfactants, $C_{12-14}H_{25-29}O(CH_2CH_2O)_9H$, from Aldrich was used in this study.

.0 g of laponite was dispersed into 200 ml of water. The suspension was stirred until it became clear. A certain amount of the PEO surfactant was added into the laponite suspension. The stirring was prolonged for 2 h to allow sufficient mixing. To this mixture, 20 ml of the Locron L solution was added drop-wise with continuous stirring. The suspension was transferred into an autoclave and maintained at 100°C for 2 days. White precipitate was recovered from the mixture by centrifuging and washed with deionized water until it is free of Cl^- ions. The wet cake was then dried in air and calcined at 500°C for 20 h. The heating temperature was raised at a rate of 2°C/min. The amounts of the surfactant added in the reaction systems were 20, 10, 4, 2 and 0 g for samples SP-I, SP-II, SP-III, SP-IV and SP-V, respectively.

2.2. Catalyst preparation

5 wt.% of Ni was loaded onto the Al-laponite supports by impregnating the supports with $Ni(NO_3)_2 \cdot 6H_2O$ solution. The suspension was stirred and heated to evaporate water and dried in an oven at 105°C overnight. The Ni-loaded supports were calcined in air at 500°C for 4 h.

2.3. Catalyst characterization techniques

The surface area and pore size of the supports and the catalysts were determined by nitrogen adsorption using a NOVA 1200 system (Quantachrom, USA) at −196°C. The sample was degassed at 300°C in vacuum before the measurement. The specific surface area was calculated using the BET method, while the pore size distribution was obtained from the desorption data by the BJH method. Total pore volume (V_t) was determined at a relative pressure $P/P_0 = 0.98$. The micropore surface area, S_{micro}, and pore volume (V_{micro}) were calculated by the t-plot method. The mesopore surface area (S_{meso}) and volume (V_{meso}) were derived by subtracting the S_{micro} and V_{micro} from the S_{BET} and V_t, respectively. The average pore size (D_p) was estimated from the pore volume assuming a cylindrical pore geometry using the equation, $R_p = 2V_{liq}/S$, where V_{liq} is the volume of liquid adsorbate contained in the pores and S is the BET surface area. CO_2 adsorption was also measured at 0°C using NOVA 1200 adsorption apparatus. The samples were degassed at 300°C for 3 h under high vacuum prior to adsorption [10].

Temperature programmed oxidation experiments of carbon species formed on the catalyst were conducted on a thermogravimetric analyzer (Shimadzu TGA-50) in air with a flow rate of 80 ml/min. The temperature was first raised to 110°C and kept for 30 min and then raised to 800°C with a heating rate of 10°C/min.

XRD powder diffraction measurements were performed on a Philips PW 1840 powder diffractometer with Co Kα radiation at 40 kV, 20 mA.

2.4. Reforming reaction

The reaction was conducted in a vertical fixed-bed reactor made of quartz tube (10 mm ID) under atmospheric pressure. 0.2 g catalyst was placed on quartz wool with the bed height of 2 mm. A thermocouple was placed in the tube with one end touching the catalyst, in order to measure the bed temperature. The stream of reactants of CH_4 and CO_2 with ratio of 1:1 was fed into the reactor at the flow rate of 60 ml/min (GHSV $= 18\,000\,cm^3/g\,h$). The analysis of the gases was carried out using on-line gas chromatograph (Shimadzu-17A) equipped with a thermal conductivity detector. A carbosphere (80–100 mesh) column was used to separate H_2, N_2, CO, CH_4 and CO_2. Prior to each reaction run, the catalyst was reduced in situ at 500°C in 10% H_2/He flow for 3 h. Methane and carbon dioxide used were of ultra high purity (>99.995%) supplied by Matheson, USA.

3. Results and discussion

3.1. Characterization of supports and catalysts

The surface areas and pore sizes of the prepared pillared clay supports and a commercial γ-Al_2O_3 are summarized in Table 1.

Support I has no micropores. All other supports contain both micropores and mesopores. The alumina intercalation greatly increases the surface area and the extent of the increase depends on the amount of the polyethylene oxide (PEO) surfactant added in the intercalating process. It is found that the BET surface area and total pore volume follows the order of SP-I > SP-II > SP-III > SP-IV > SP-V > γ-Al_2O_3.

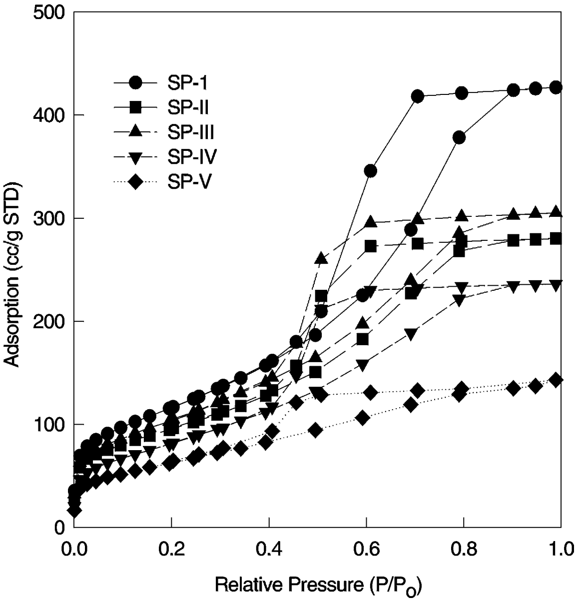

Fig. 1. N_2 adsorption/desorption isotherms of Ni catalysts supported on Al-laponite supports.

N_2 adsorption/desorption isotherms of Al-laponite are shown in Fig. 1. It is seen that the isotherm for support SP-V exhibits a shape of type IV isotherm with a hysteresis of type H4 [10]. However, the adsorption at low relative pressures is high with respect to the total adsorption. It reflects that micropores account for the majority of the pore volume in the clay and the mesopores contribute the rest [11]. Supports SP-II, -III and -IV exhibit also an isotherm of type IV but with much higher sorption volume from mesopores. Support I exhibits virtually no micropores but only mesopores in this solid.

The thermal stability of the supports was investigated upon calcination at high temperatures. The

Table 1
Surface areas and mean pore sizes of alumina intercalated laponite supports and alumina

Supports	S_{BET} (m^2/g)	S_{micro} (m^2/g)	S_{meso}	D_p (Å)	V_t (cm^3/g)
SP-I	531.35	0	531.35	73.51	0.977
SP-II	444.08	123.44	320.64	47.75	0.542
SP-III	436.59	111.25	325.34	49.64	0.530
SP-IV	416.76	140.62	276.14	45.08	0.470
SP-V	278.28	141.70	136.58	36.43	0.253
γ-Al_2O_3	145.0	–	–	55.00	0.250

Table 2
Pore structure characteristics of SP-I sample heated at various temperatures

	Temperature (°C)			
	500	600	700	800
S_{BET} (m^2/g)	531.35	397.65	376.51	199.91
V_t (cm^3/g)	0.977	0.493	0.466	0.341
D_p (nm)	73.51	49.67	49.51	68.31
S_{meso} (m^2/g)	531.35	201.99	200.37	163.8
V_{meso} (cm^3/g)	0.977	0.404	0.388	0.323
S_{micro} (m^2/g)	0.00	195.65	176.14	36.08
V_{micro} (cm^3/g)	0.00	0.089	0.078	0.018

surface areas and porosity data of the SP-I after the heat treatments are shown in Table 2.

It is seen that the porosity of intercalated clay seriously reduced with increasing treatment temperature in terms of S_{BET}, V_t, V_{meso} and S_{meso}. For instance, SP-I sample calcined at 500°C lost about 62% of its BET surface area during the heat treatment at 800°C. Thermal treatment at high temperatures, in particular, above 700°C has strongly affected the mesopore structure of the intercalated clays. It is known that clay layers are generally unstable above 700°C [12,13]. The damage to the clay layers inevitably results in the collapse of the pore structure in the intercalated derivatives of the clay.

The textural parameters of the Ni catalysts prepared on these clay supports as prepared and after reforming reaction for 140 h are shown in Table 3.

The catalysts show similar patterns of porous structure as the supports in Table 1. The surface areas decreased appreciably in most catalysts relative to the supports due to the loading of nickel.

Laponite exhibits obvious basic property, the pH of its suspension is over 9. It is anticipated that the pore surface of the intercalated supports has a strong ability to adsorb CO_2. CO_2 adsorption on these solids was measured at 0°C. We found that CO_2 adsorption by the intercalated laponite is dependent on the surface area and significantly greater than that by commercial γ-alumina. CO_2 adsorption on Al-laponite also increases with increasing porosity, which is conformed by the results of the other studies [14]. After the reaction, the surface areas of used catalysts are sharply decreased.

3.2. Catalytic activity and stability for CO_2 reforming of methane

3.2.1. Catalysts activity

The catalytic performance of all catalysts was evaluated for CO_2 reforming of methane in a fixed-bed reactor in the temperature range 500–900°C. Fig. 2 shows the initial conversions of methane and carbon

Table 3
Characteristics of Ni/Al-laponite catalysts as prepared and after reforming reaction for 140 h

S_{BET} catalysts	S_{meso} (m^2/g)	S_{micro} (m^2/g)	V_t (m^2/g)	CO_2 (cm^3/g)	Adsorption (mmol/g cat.)
Ni/SP-I					
Fresh	421.48	299.42	122.06	0.66	0.37
Used	250.89	240.99	9.9	0.49	
Ni/SP-II					
Fresh	345.50	200.42	145.10	0.43	0.37
Used	210.70	192.98	17.72	0.34	
Ni/SP-III					
Fresh	378.35	193.85	184.50	0.47	0.35
Used	199.95	185.64	14.3	0.34	
Ni/SP-IV					
Fresh	298.49	104.53	193.95	0.36	0.29
Used	107.70	74.99	32.71	0.17	
Ni/SP-V					
Fresh	228.14	126.61	101.54	0.22	0.24
Used	10.41	10.41	–	0.02	

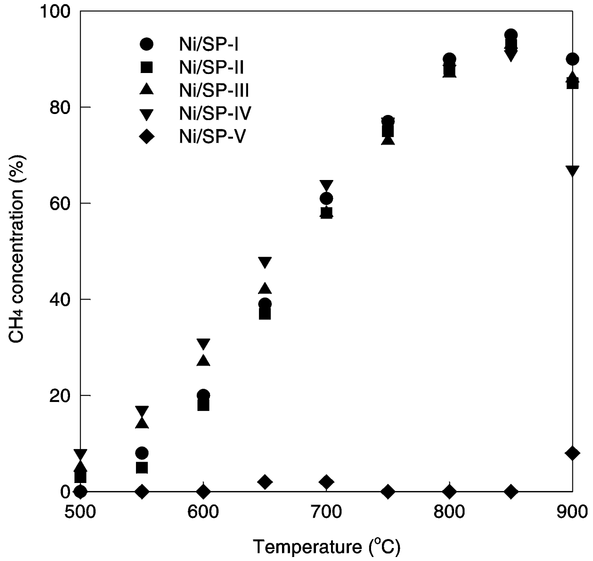

Fig. 2. Conversions of CH_4 over various catalysts as a function of reaction temperature. Reaction condition: $CH_4/CO_2 = 1{:}1$, $P = 1$ atm.

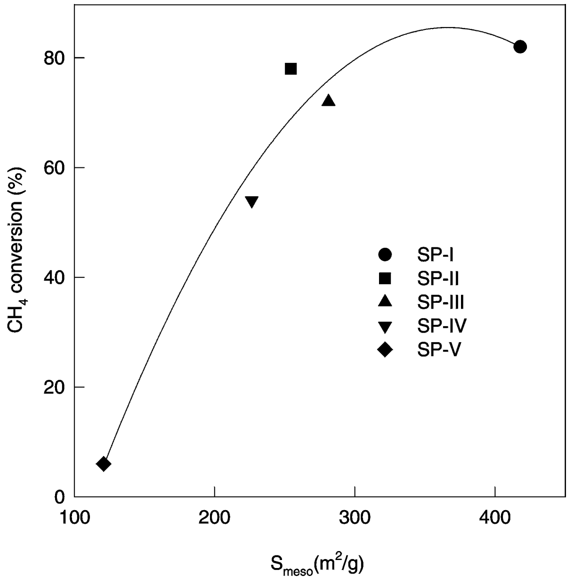

Fig. 3. Relationship between CH_4 conversion and S_{meso} of the Ni/Al-laponite catalysts.

dioxide at the different reaction temperatures. These results indicate that the use of nickel catalysts supported on Al-laponite results in good activity for CH_4 conversion. It is obvious that the conversion increases with the rise of the reaction temperature except for Ni/SP-V catalyst. It is thought that carbon deposition on catalyst V is more severe than on any other catalyst (see Fig. 5). The porosity and pore size of this catalyst is much lower compared to the others. In addition, the intercalated pore structure of the catalyst almost completely collapses during the reaction. These are probably the reasons why this catalyst deactivated faster This figure also shows that the activity of nickel supported on Al-laponite is similar to the nickel catalyst supported on γ-Al_2O_3. The extent of the increase of conversion depends on the surfactant amount added into the laponite suspension. The best sample is Ni/SP-IV that is very close to that of Ni/Al_2O_3.

We also found that the CH_4 conversions at 900°C were lower at 850°C. The drop in CH_4 conversion at 900°C is believed to be the consequence of sintering and collapsing of the support clay structure, which was reflected in the physical characteristics as shown in Table 3.

Some researchers have shown that the pore structure affected the catalyst activity in CO_2 reforming of methane [15–17]. The surface area from mesopores of catalysts is found to show significant effect on CH_4 conversion.

The textural properties of supports influence the catalytic activity in two ways: (1) highly dispersed active sites are formed on the supports of large mesopore surface areas; (2) accessibility of reactants to active sites is high on mesoporous supports and thus result in high reactivity. Fig. 3 shows the relationship between CH_4 conversion at 800°C and the mesopore area, S_{meso} of catalysts. CH_4 conversion is strongly dependent on the mesopore area, S_{meso}. It appears that most of the active sites for the reaction are located on the surface of mesopores.

The surface properties of a catalyst also affect the catalytic activity. Some studies have indicated that the addition of basic promoters improves the catalytic activity of dry reforming of carbon dioxide with methane. CO_2 reforming of methane involves the adsorption of CO_2 [18,19]. Strong ability to adsorb CO_2 enhances the rate of surface reaction of the active carbon species and thus stimulates the reaction. The results of CO_2 adsorption on catalysts have demonstrated that the larger surface area allows for higher CO_2 adsorption capacity (see Table 3). The low porosity decreased the amount of contact that the gas had with the catalyst surface and thus a lower conversion resulted in.

3.2.2. Catalysts stability

The temperature dependence of the deactivation process was investigated at 800°C over Ni/γ-Al_2O_3 catalyst and Ni/Al-laponite catalyst, respectively (Fig. 4). It is seen that all catalysts showed deactivation of different extents. As clearly shown in Fig. 2, CO_2 conversions decreased faster between 1–5 h and then the variation in CO_2 conversion tended to be small. The primary reasons for deactivation of Ni catalysts can be generally ascribed to carbon deposition on the nickel crystallites and the sintering of nickel particles. The ratio of the CO_2 conversion at 140 h to that at 2 h is used as indicative of deactivation. It is found that catalyst Ni/SP-IV deactivated faster, whereas catalysts Ni/SP-III exhibited a slower deactivation. Over catalysts Ni/SP-I and Ni/SP-II, the ratio are about 95 and 88%, respectively, showing relative stable activity. It has been evidenced that the content of carbon deposition differs widely on carbon dioxide reforming reaction and carbon deposition mainly depending on the supports. The deactivation rates of catalysts Ni/SP-I, Ni/SP-II and γ-Al_2O_3 are very slow but catalysts Ni/SP-IV was deactivated seriously in 1 day. The catalyst Ni/SP-III was quickly deactivated after 100 h. Carbon deposition experiments on these catalysts also demonstrate that coking is more severe on catalyst Ni/SP-V than that on other supported catalysts. The above results suggest that Ni/(Al-laponite) catalyst shows not only high activity

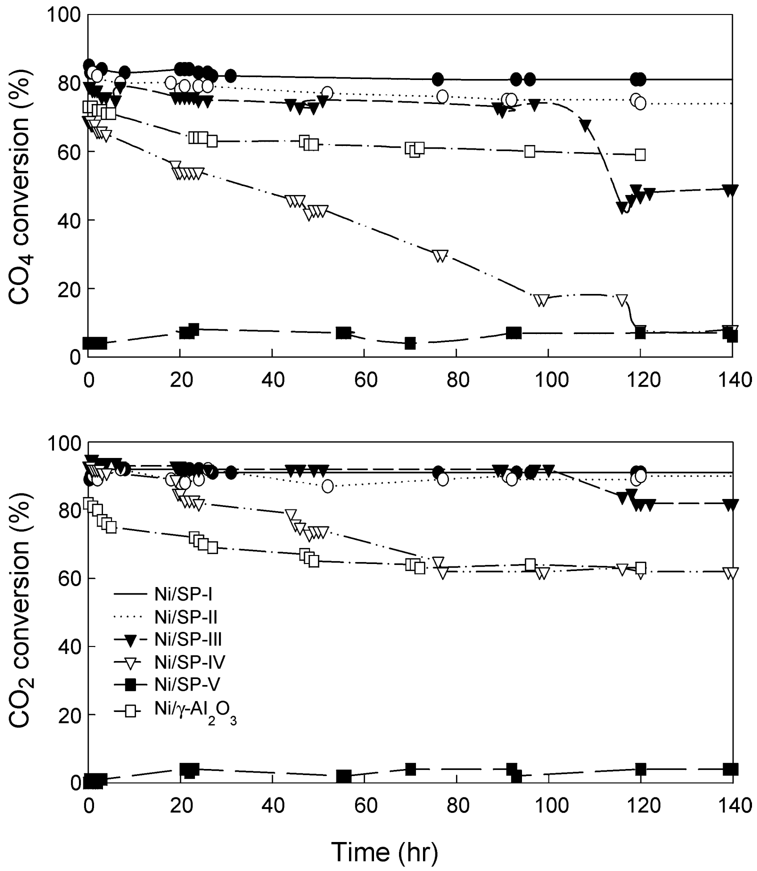

Fig. 4. Stability of Ni catalysts supported on Al-laponite and alumina (Ni loading 5%; reaction conditions: CH_4:CO_2 = 1:1 P = 1 atm, flow rate = 60 ml/min).

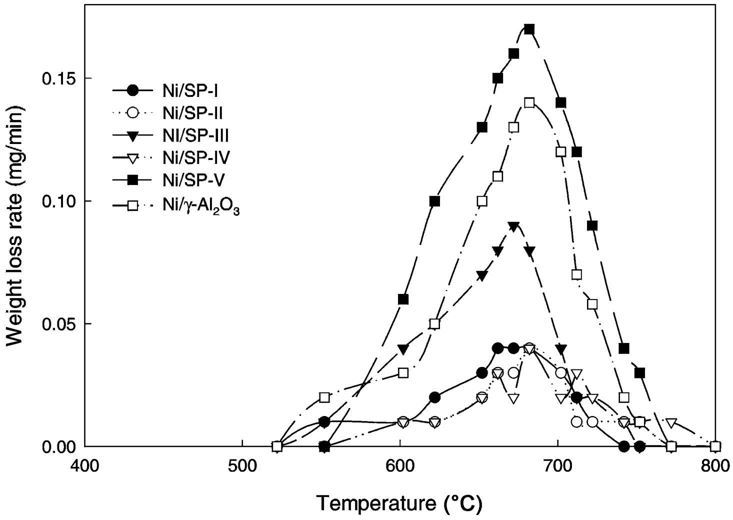

Fig. 5. TPO profiles of carbonaceous species formed on the catalyst after reaction for 140 h at 800°C.

but also a longer stability, particularly those supports made with high amounts of surfactants. After a long reaction time of 140 h, CO_2 and CH_4 conversion over catalyst Ni/SP-I and Ni/SP-II only decreased by about 5 and 8%, respectively This is much better than the drop in conversions over Ni/Al_2O_3 catalyst, which are, respectively, 13.5 and 18.2%, at 140 h.

The amount of carbon deposited on the catalysts in deactivation tests was measured by temperature programmed oxidation (TPO) experiments in a TGA. The weight loss profile and the percentage loss between 500 and 800°C is presented in Fig. 5. From the figure, it is seen that carbon began to be oxidized at 520°C but their peaks occurred at different temperatures. Carbon on Ni/SP-I showed the maximum oxidation rate around 670°C and the oxidation of carbon on Ni/SP-V catalyst showed a peak at about 690°C. For $Ni/\gamma\text{-}Al_2O_3$ catalysts, carbon was also to be oxidized with the peaks occurring around 690°C. The amount of carbon results indicated that the Ni/SP-I and Ni/SP-II catalysts had the lower coking activity, while Ni/SP-V and $Ni/\gamma\text{-}Al_2O_3$ catalyst showed higher coking among the six tested catalysts. Swaan et al. [20] reported that there were two types of carbon deposited on Ni/Al_2O_3 catalyst. They were oxidized at 500 and 650°C, respectively. Considering the location of carbon and nickel particles and the gasfication temperature, it can be deduced that surface carbon species were easily gasified. Several researches [17] have shown that there is a relationship between oxidation temperature and the location of carbon on the support and the metal. Coke on the metal is burned at a lower temperature than the coke on the support because metals can catalyze the coke combustion in air. It can be seen that the coke formed

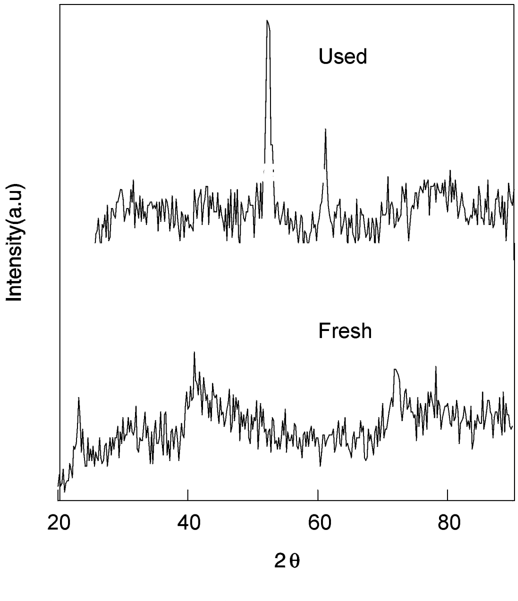

Fig. 6. XRD patterns of fresh and used catalysts (Ni/SP-I).

on catalysts Ni/SP-I and Ni/SP-II are mostly located on the Ni metal which is believed to be nanotube carbons, whilst the coke formed on other catalysts are more amorphous carbons resulting in quick deactivation of the catalysts. The nanotube carbon grows very slowly leading to a slow deactivation process.

The XRD patterns of the fresh and used catalysts (catalysts I) are shown in Fig. 6. It is seen that no nickel diffraction is observed on the fresh catalyst. However, the nickel peaks appear on used catalyst. This is indicative of the occurrence of Ni sintering. The metal sintering was also found on other Ni/clay catalysts in this investigation.

4. Conclusions

Alumina intercalated laponite is a promising support for catalysts for carbon dioxide reforming of methane. Pore structures and surface nature of these solids can be tailored to obtain high surface area that allows a good dispersion of nickel catalyst. The BET surface area increases with increasing concentration of surfactant added in the clay suspension.

For CO_2 reforming of methane over the catalysts supported on the Al-laponite, the optimum condition to obtain high conversion is around 800°C. Carbon deposition on these catalysts demonstrates that coking is more severe on the catalysts of low porosity (catalyst V) than on the catalysts of high porosity.

Acknowledgements

This work has been supported by KOSEF under Oversea Post-Doctorate Program. Financial support from the Australian Research Council (ARC) and the University of Queensland are gratefully acknowledged. HYZ is indebted to ARC for the QE II fellowship.

References

[1] J.R. Rostrup-Nielsen, Stud. Surf. Sci. Catal. 81 (1994) 25–41.
[2] D.M. Bibby, C.D. Chang, R.F. Howe, S. Yurchak, Methane Conversion, Elsevier, Amsterdam, 1988.
[3] J.H. Edwards, A.M. Maitra, Natural Gas Conversion II, Elsevier, Amsterdam, 1994, pp. 291–296.
[4] K. Ohtsuka, Chem. Mater. 9 (1997) 2039–2050.
[5] T.J. Pinnavaia, Intercalated clay catalysts, Science 220 (4595) (1983) 365–372.
[6] R. Burch, Catalysis Today, Vol. 2, Elsevier, New York, 1988.
[7] H.Y. Zhu, S. Yamanaka, J. Chem. Soc. Faraday Trans. 93 (1997) 477–480.
[8] S. Wang, Ph.D. Thesis, University of Queensland, 1998.
[9] S. Wang, H.Y. Zhu, G.Q. Lu, J. Colloid Interf. Sci. 204 (1998) 128–134.
[10] H.Y. Zhu, C.Q. Lu, G.Q. Lu, Langmuir (2001), in press.
[11] S.J. Gregg, K.S.W. Sing, Adsorption, Surface Area and Porosity, 2nd Edition, Academic Press, New York, 1982.
[12] M.L. Occelli, Ind. Eng. Chem. Prod. Res. Dev. 22 (1983) 553.
[13] H.Y. Zhu, J.A. Xia, E.F. Vansant, G.Q. Lu, J. Porous Mater. 4 (1997) 17.
[14] L.M. Gandia, R. Toranzo, M.A. Vicente, A. Gil, Appl. Catal. A 183 (1999) 23–33.
[15] A.M. Gadalla, B. Bower, Chem. Eng. Sci. 42 (1988) 3042.
[16] W.Y. Li, K.C. Xie, S.C. Xie, Coal Sci. Technol. 24 (1995) 727.
[17] S. Wang, G.Q. Lu, Appl. Catal B 16 (1998) 269.
[18] C.Y. Wang, S.Y. Yang, X.R. Li, J. Ren, Y.G. Chen, Energy Convers. Mgmt. 37 (1996) 1357.
[19] Z.X. Cheng, Q.L. Wu, J.L. Li, Q.M. Zhu, Catal. Today 30 (1996) 147.
[20] H.M. Swaan, V.C.H. Kroll, G.A. Martin, C. Mirodatos, Catal. Today 21 (1994) 571–578.